

CLASSICAL BILLIARDS CAN COMPUTE

EVA MIRANDA AND ISAAC RAMOS

ABSTRACT. We show that two-dimensional billiard systems are Turing complete by encoding their dynamics within the framework of Topological Kleene Field Theory. Billiards serve as idealized models of particle motion with elastic reflections and arise naturally as limits of smooth Hamiltonian systems under steep confining potentials. Our results establish the existence of undecidable trajectories in physically natural billiard-type models, including billiard-type models arising in hard-sphere gases and in collision-chain limits of celestial mechanics.

Significance statement. Billiards are a textbook model of deterministic motion: a particle moves freely and reflects specularly from rigid walls. We show that, even in two dimensions, billiard trajectories can simulate arbitrary Turing machines. This universality implies a sharp limit on prediction: there is no general algorithm that can decide basic questions such as whether a trajectory is periodic. Because billiards also arise as limits of smooth Hamiltonian systems with increasingly steep confining potentials, these algorithmic barriers are not confined to idealized hard-wall models. Our results place undecidability, alongside chaos, as a fundamental obstruction to long-term prediction even in low-dimensional classical dynamics.

1. INTRODUCTION

Billiards are among the simplest dynamical systems: a point particle moves freely inside a domain and undergoes specular reflection at the boundary. Since Birkhoff's formulation of the billiard map, they have served as canonical models for Hamiltonian and symplectic dynamics with singular interactions [4, 5]. Despite their elementary definition, billiards exhibit an extraordinary range of behaviors, from complete integrability to strong chaos. Sinai's dispersing billiards provided foundational examples of hyperbolic and ergodic dynamics [29], while polygonal billiards connect to flat geometry, translation surfaces, and Teichmüller dynamics [24, 22].

Billiards also play a central role in physics. In kinetic theory, systems of hard spheres are equivalent to billiard flows in configuration space [14]. In quantum mechanics, quantum billiards model systems such as quantum dots and microwave cavities, where a particle is confined by rigid boundaries, and in the semiclassical regime many features of the quantum dynamics are determined by the geometry and trajectories of the corresponding classical billiard [3, 20, 21]. Importantly, billiards can be realized as limits of smooth Hamiltonian systems by replacing hard walls with steep confining potentials that diverge near the boundary. In this soft-wall limit, smooth Hamiltonian flows converge (excluding trajectories that hit the boundary nearly tangentially) to billiard motion, allowing billiard results to be interpreted within standard classical mechanics.

Given the richness of billiard dynamics, a natural question arises: can billiards realize the full complexity of computation? Since the pioneering work of Moore [25, 26], it has become clear that

Both authors are partially supported by the project “Computational, dynamical and geometrical complexity in fluid dynamics” (COMPLEXFLUIDS), Ayudas Fundación BBVA a Proyectos de Investigación Científica 2021. Eva Miranda is supported by the Catalan Institution for Research and Advanced Studies via an ICREA Academia Prize 2021 and by the Alexander Von Humboldt Foundation via a Friedrich Wilhelm Bessel Research Award. Miranda is also supported by the Spanish State Research Agency, through the Severo Ochoa and María de Maeztu Program for Centers and Units of Excellence in R&D (project CEX2020-001084-M) and both authors are supported by the project PID2023-146936NB-I00 by the Spanish State Research Agency MCIU/AEI / 10.13039/501100011033/ FEDER, UE. Miranda thanks the FIM at ETHZ Zurich for their hospitality during her stay in Zürich as Nachdiplom lecturer in the Fall Semester of 2025 when this article was written. Isaac Ramos is supported by a fellowship from “La Caixa” Foundation (ID 100010434) with code LCF/BQ/PFA25/11000070.

many continuous dynamical systems can simulate algorithms and thereby exhibit undecidability phenomena rooted in Turing's Halting problem [31]. At a more foundational level, the question of whether physical systems can genuinely realize such Turing-universal behavior has been central since the very origins of computation, notably in the seminal works of Feynman [15] and Wolfram [33]. Universal computation has since been embedded in a wide range of settings, including polynomial differential equations, mechanical systems with tailored potentials, cellular automata and hydrodynamic flows [23, 19, 8, 32, 34, 30, 9, 12, 13, 11, 10, 18]. A unifying framework behind several of these results is Topological Kleene Field Theory, which encodes computable functions into flows on manifolds with boundary so that dynamical questions translate into questions of computation [17].

Within this program, billiards present a stringent test case. Moore suggested that billiard systems in sufficiently high dimension, most notably three-dimensional billiards, could support universal computation, while also arguing that genuinely low-dimensional systems might lie below the universality threshold [25, 26]. Subsequent work achieved Turing completeness for billiard-like models by adding dynamical ingredients such as many-ball systems [16], three-dimensional walls [28], and moving walls or internal memory encoded in the particle's velocity, for example, in computational pinball machines [1]. *Here we show that classical planar billiards with one ball and fixed walls already realize universal computation, achieving Turing completeness in physical systems with only one-degree of freedom.*

We adapt the machinery of Topological Kleene Field Theory to billiard flows and, for each Turing machine, construct a two-dimensional billiard table whose trajectories simulate its computation. As a consequence, natural decision problems for planar billiards, including reachability and periodicity questions, are algorithmically undecidable. Our approach is based on an encoding that is compatible with billiard geometry. We encode computation states as points of a one-dimensional interval and let the tape head move rather than shifting the entire tape. In our realization, the shift arises naturally from reflections on parabolic walls, while the read–write operation is more involved but remains fully compatible with a physical billiard system.

Beyond its intrinsic mathematical interest, Turing completeness in planar billiards has broader implications. Because billiards arise as hard-wall limits of smooth Hamiltonian systems, undecidability in billiards points to intrinsic algorithmic limits in certain steep potential Hamiltonian dynamics. Moreover, billiard-type descriptions appear effectively in several physical regimes, including hard sphere gases and collision-dominated limits in celestial mechanics, suggesting that undecidability may emerge naturally in physically motivated models. In particular, several models in celestial mechanics admit billiard descriptions near close encounters, including variants of the three-body problem. Because the Halting problem is undecidable, our results imply undecidability for families of billiard-type models that arise as effective descriptions of close-encounter dynamics. This suggests that collision-dominated regimes in celestial mechanics may exhibit qualitative behaviors that cannot be decided algorithmically, even when the underlying equations are deterministic. This provides a first indication that undecidability may arise in classical celestial mechanics, alongside chaos, as a fundamental obstruction to long-term prediction, with potential consequences for questions of stability and ejection in planetary systems.

Outline. Section 2 reviews billiards and Turing machines. Section 3 presents the construction of computational billiards and proves Turing completeness. Section 4 discusses consequences and physical interpretations. Section 5 presents some conclusions.

Acknowledgements: We thank FIM and ETH Zürich for providing an ideal environment for this collaboration. We are also grateful to Stephen Wolfram for his visit in October 2025, which inspired several related questions that ultimately led to this work. We further thank Ángel González-Prieto for insightful discussions that shaped our encoding of the computational states of a Turing machine into a one-dimensional interval. We also thank John Baez and Joel David Hamkins for their interest.

2. PRELIMINARIES

2.1. Billiards. Planar billiards describe the motion of a point particle undergoing free flight,

$$\ddot{q}(t) = 0,$$

with elastic reflections at the boundary of a domain $B \subset \mathbb{R}^2$,

$$v^+ = v^- - 2\langle v^-, n \rangle n,$$

where n denotes the inward unit normal. Despite their elementary definition, billiards arise ubiquitously in physics as exact or effective models for systems with hard constraints, singular interactions, or piecewise smooth dynamics.

Depending on the geometry and regularity of the boundary ∂B , one distinguishes several important classes of billiards, such as polygonal billiards with piecewise linear boundary and smooth billiards including elliptic tables. More generally, one often assumes that ∂B is piecewise smooth, or of class C^k . In this article, we work within this general setting.

2.2. Turing machines. This celebrated computability model captures the essence of a computer from a mathematical point of view. Due to its intuitive formulation, it has become one of the most standard and widely adopted models of computation. Formally, a (binary) Turing machine consists of a tuple

$$M = (Q, q_0, Q_{\text{halt}}, \delta),$$

where Q is a finite set, whose elements are the *states* of M , $q_0 \in Q$ is the *initial state*, $Q_{\text{halt}} \subsetneq Q$ is the subset of *halting states*, and

$$\delta : Q \times \mathcal{A} \rightarrow Q \times \mathcal{A} \times \{-1, 1\}$$

is the *transition function*. Here $\mathcal{A} = \{0, 1\}$ is the tape alphabet.

From this information, we can define a dynamical system. Let $\Lambda \subset \mathcal{A}^{\mathbb{Z}}$ be the set of finite two-sided sequences $t : \mathbb{Z} \rightarrow \mathcal{A} = \{0, 1\}$. We refer to each $t \in \Lambda$ as a *tape state*. The set of computation states \mathcal{S} consists of words of the form

$$\mathcal{S} = \{(t, q, k) \in \Lambda \times Q \times \mathbb{Z}\}$$

where $t \in \Lambda$ is a tape state, $q \in Q$ is the current internal state of the machine and $k \in \mathbb{Z}$ is the position of the head¹. At certain points in our construction, when q is not relevant, we will abuse terminology and refer to (t, k) alone as the computation state. We then define

$$\Delta_M : \mathcal{S} \rightarrow \mathcal{S}$$

by the following rule. Given a computation state (t, q, k) , the Turing machine evaluates $\delta(q, t_k) = (q', s, \varepsilon)$ and sets $\Delta_M(t, q, k) = (t', q', k + \varepsilon)$, where the new tape t' satisfies

$$t'_n = t_n \quad \text{for } n \neq k, \quad t'_k = s.$$

The map Δ_M encodes the intuitive idea that t represents a two-sided tape, and M has a read–write head currently positioned at cell k . At each iteration, the head reads the symbol underneath it, and based on the present internal state q of the machine, it writes a new symbol s on the tape, moves either left ($\varepsilon = -1$) or right ($\varepsilon = 1$), and updates the internal state to q' . In this way, for a given initial tape t , the map Δ_M generates a dynamical system on \mathcal{S} starting from $(t, q_0, 0) \in \mathcal{S}$. If, at some point, the system reaches a configuration (t', q', k') with $q' \in Q_{\text{halt}}$, the computation is said to halt.

In the following section, we will see that the reversibility condition is essential for building well-structured dynamical systems capable of simulating universal computation. The reversibility of

¹Notice that the standard definition of a Turing machine does not include the position of the head in the computation state. Instead, it always assumes that the head is at position 0 and when shifting, it moves the entire tape in the opposite direction instead of displacing the head. However, we have decided to use this definition, which is also more intuitive, because it makes our encoding of the Turing machine into a billiard system easier to understand.

a Turing machine can be defined in several equivalent ways. For our purposes, the formulation based on the global transition function δ is the most convenient.

Definition 1. A Turing machine $M = (Q, q_0, Q_{\text{halt}}, \delta)$ is *reversible* if the global transition function Δ_M is injective.

In the seminal paper [2], Bennett demonstrated that any computation can be carried out by a reversible Turing machine, as stated in the following theorem.

Theorem 1. [2] *For every Turing machine, there exists an equivalent reversible Turing machine.*

Hence, focusing exclusively on reversible Turing machines does not impose any real restriction.

There is a geometric perspective for interpreting Turing machines as graphs, commonly called *finite state machines*. Consider a Turing machine

$$M = (Q, q_0, Q_{\text{halt}}, \delta).$$

We associate to M a finite state machine \mathcal{G}_M , defined as the following labelled directed graph:

- The vertices of \mathcal{G}_M are the states Q of M .
- Each non-halting state $q \notin Q_{\text{halt}}$ has two outgoing edges connecting to the new states determined by the transition function,
- The halting states in Q_{halt} are represented as vertices with no outgoing edges.

The finite state machine \mathcal{G}_M corresponding to the Turing machine M thus provides a graphical representation of the evolution of M 's internal states during a computation. The computation begins at the initial vertex q_0 and, at each step, the system moves along the edge determined by the symbol currently read on the tape, updating the tape and shifting the head left or right according to the label of that edge. As we will explain in the proof of the main theorem, we will use this geometrical representation to encode any Turing machine as a billiard flow.

3. TURING COMPLETENESS OF TWO-DIMENSIONAL BILLIARDS

The key tool for building a dynamical system capable of simulating a Turing machine is symbolic dynamics. In this section we explain how to adapt Moore's framework [25] and the Topological Kleene Field Theory construction [17] for two-dimensional billiard dynamics.

3.1. Cantor-based encodings. The standard ternary Cantor set is the set of real numbers $x \in \mathbb{R}$ that can be written as

$$x = \sum_{i=1}^{\infty} \epsilon_i 3^{-i}, \quad \epsilon_i \in \{0, 2\}.$$

This Cantor set provides a way to encode sequences of natural numbers on the unit interval.

Following this idea, we introduce a convenient map that encodes tape states over the alphabet $\mathcal{A} = \{0, 1\}$ as points of the closed interval $I = [0, 1] \subset \mathbb{R}$. Let $t = \{t_n\}$ be a tape state with $t_n \in \mathcal{A}$ for all $n \in \mathbb{Z}$. We assign to t the point in the Cantor set

$$x_t = 2 \sum_{n=0}^{\infty} t_n 3^{-(2n+1)} + 2 \sum_{n=1}^{\infty} t_{-n} 3^{-2n} = 2(t_0 3^{-1} + t_{-1} 3^{-2} + t_1 3^{-3} + \dots).$$

Here, we have used the elements of t as the ternary digits of our point in I , by alternating elements of the positive half of tape, $\{t_n\}_{n \geq 0}$, with those of the negative half, $\{t_n\}_{n < 0}$. In other words, the right- and left-hand sides of the tape t are encoded in the odd and even digits of the ternary expansion of x_t , respectively.

We would also like to add somehow the information about the position of the head into this encoding. In order to do so, we will embed a smaller copy of I into itself for each $k \in \mathbb{Z}$ via an affine map $\tau_k : I \hookrightarrow I$. By having the length of $I_k := \tau_k(I)$ decrease fast enough as $|k|$ goes to infinity, we can construct these embeddings so that the intervals I_k are pairwise disjoint. If we also assume that I_k is to the left of $I_{k'}$ if $k < k'$ and we have symmetry with respect to the center of the interval, the result we obtain looks like the one in Figure 1. Using these intervals,

we can encode the tape t when the head state is at position k as the point $x_{t,k} := \tau_k(x_t) \in [0, 1]$.

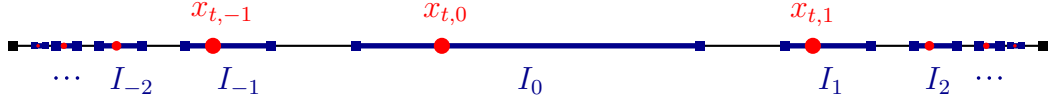


FIGURE 1. Encoding into the one-dimensional interval. Each interval represents a position of the head and the tape state is represented by a point in the interval.

3.2. Embedding Turing machines into billiards.

Definition 2 (Computational billiard). A computational billiard is a triple $(B, \iota_0, \iota_{\text{halt}})$, where B is a billiard table, and $\iota_0, \iota_{\text{halt}} : I \hookrightarrow \partial B$ are embeddings of the interval I into the boundary of the billiard.

The idea of our construction is to associate an initial tape t of a Turing machine to a point $p_0 \in \partial B$ by applying the embedding ι_0 to $x_{t,0}$ (assuming the head is initially at position 0). Then, we let this point move through the billiard by shooting it in the direction perpendicular to the boundary. If it hits the point $p_{\text{halt}} := \iota_{\text{halt}}(x_{t',k})$ orthogonally, we interpret this as the Turing machine halting, with t' being the output tape.

Remark 1. Notice that in the previous situation, after hitting p_{halt} , the billiard ball bounces off and travels backward until it returns to p_0 . Therefore, the halting of the Turing machine implies the periodicity of the billiard trajectory.

The billiard trajectory may start at a point $\iota_0(x_{t,0})$ and never reach the interval $\iota_{\text{halt}}(I)$, or if it does reach it, it does not hit orthogonally a point of the form $\iota_{\text{halt}}(x_{t',k})$. We interpret this situation as the Turing machine not halting for the input tape t .

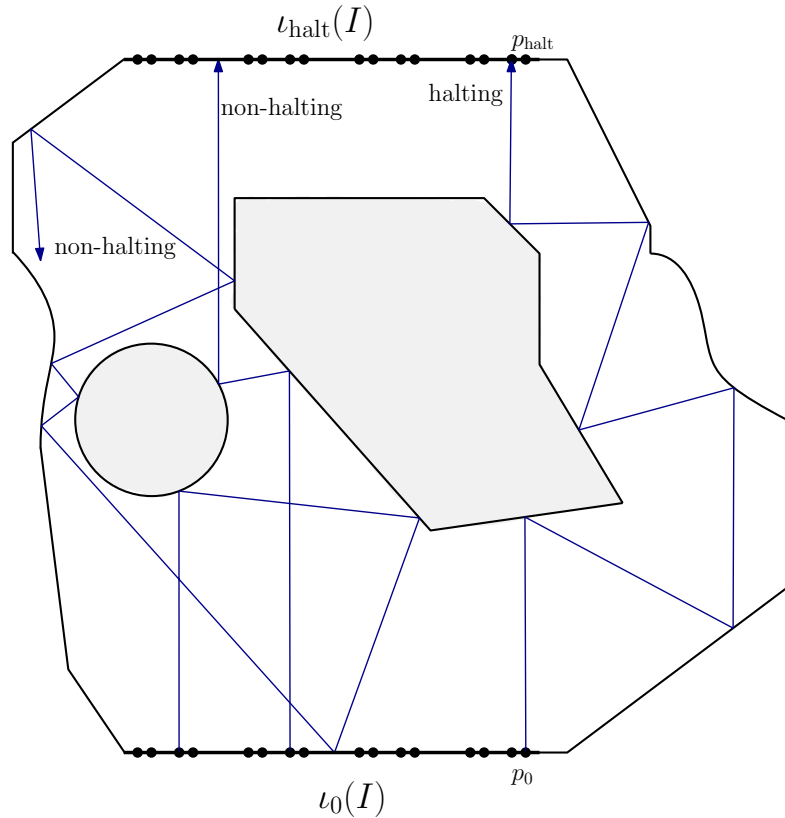


FIGURE 2. Different trajectories of a computational billiard.

Using these ideas, we can formulate our main result:

Theorem 2. Two-dimensional billiard systems are Turing complete, in the sense that for each Turing machine we can find a computational billiard $(B, \iota_0, \iota_{\text{halt}})$ associated with it.

In order to prove this theorem, we will adapt the construction of computational bordisms in the framework of Topological Kleene Field Theory [17] to the case of billiards. In this proof, we deeply exploit an alternative representation of a Turing machine as a finite state machine. As we previously discussed, given a Turing machine T , we can express it as a directed finite graph where its nodes correspond to the states of T and the edges represent the simple operations performed by the machine at each step. Encoding the tape and head position as a point in the interval through the Cantor set-like embedding, we prove that these simple operations can be implemented using explicit billiard-like dynamics.

More concretely, we transform the graph representing T into a billiard table. The computation states corresponding to the initial and halting states are encoded in the walls of the billiard table via ι_0 and ι_{halt} , respectively, and represent the initial and final positions of the computation. Each edge of the graph is represented by a “corridor” in the billiard table, along which the billiard dynamics replicate the operations performed by that edge.

The remaining nodes of the graph, corresponding to intermediate states of the Turing machine, are encoded by “checkpoint” intervals $\iota_i(I)$ associated with the state q_i . In this way, the billiard trajectory passes through the point $\iota_i(x_{t,k})$ precisely when the current computation state is (t, q_i, k) . See Figure 3 for a sketch of a simple Turing machine transformed into a computational billiard.

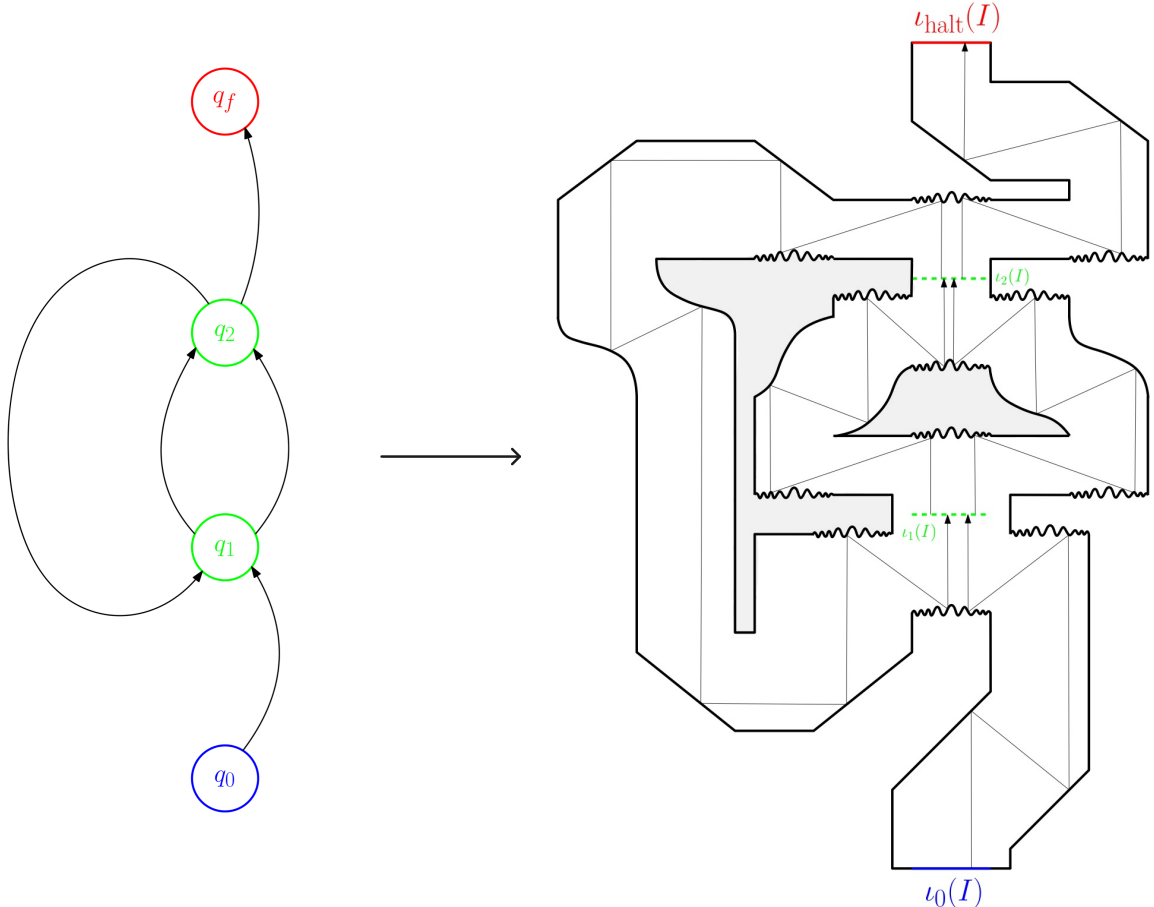


FIGURE 3. Transforming the graph representation of a Turing machine into a billiard.

Remark 2. Notice that using this proof method, the computational billiard created has as strong deformation retract the graph of the associated Turing machine. In particular, our construction requires a billiard table with a non-trivial topology, where we place an obstacle in the billiard

for each of the generators of the fundamental group of the graph. In this context, one may ask the following question: is it possible to construct a computational billiard whose number of obstacles is strictly less than the first Betti number of the graph corresponding to the associated Turing machine? This is reminiscent of the connection between computational complexity and topological complexity. See also [17].

3.3. Proof of the main theorem. In this section, we shall prove Theorem 2 by showing that any finite state machine can be represented through a computational billiard. We prove that the basic operations performed by each edge of the finite state machine, namely shifting the head and reading or writing a symbol, can be realized through billiard-like dynamics. The result will then follow by constructing a billiard table based on the graph of the associated Turing machine, where we use these dynamics at each of the “corridors” representing the edges.

Lemma 1. *The shift operation can be realized through billiard-like dynamics.*

Proof. Using our encoding of the computation states into the one-dimensional interval, shifting the head becomes equivalent to mapping the points $x_{t,k}$ to $x_{t,k+\varepsilon}$ with $\varepsilon = -1, 1$. We can assume without loss of generality that $\varepsilon = 1$, and prove that we can find some billiard walls that implement these dynamics.

We will use an explicit expression for the embeddings $\tau_k : I \hookrightarrow I_k \subseteq I$:

$$\tau_k(x) = \begin{cases} 3^{-(1-k)}(1+x), & k < 0, \\ 1 + 3^{-(1+k)}(-2+x), & k \geq 0. \end{cases}$$

Notice that using these embeddings, each interval I_k has length $3^{-(1+|k|)}$ and they are all disjoint. Moreover, for any tape t

$$x_{t,k+1} = \begin{cases} 3x_{t,k}, & \text{if } k < 0, \\ x_{t,k}/3 + 2/3, & \text{if } k \geq 0. \end{cases}$$

These are affine transformations that can be realized using billiard walls with the form of parabolas sharing a common focus, as suggested in [25] for the three-dimensional billiard setting and illustrated in Figure 4. \square

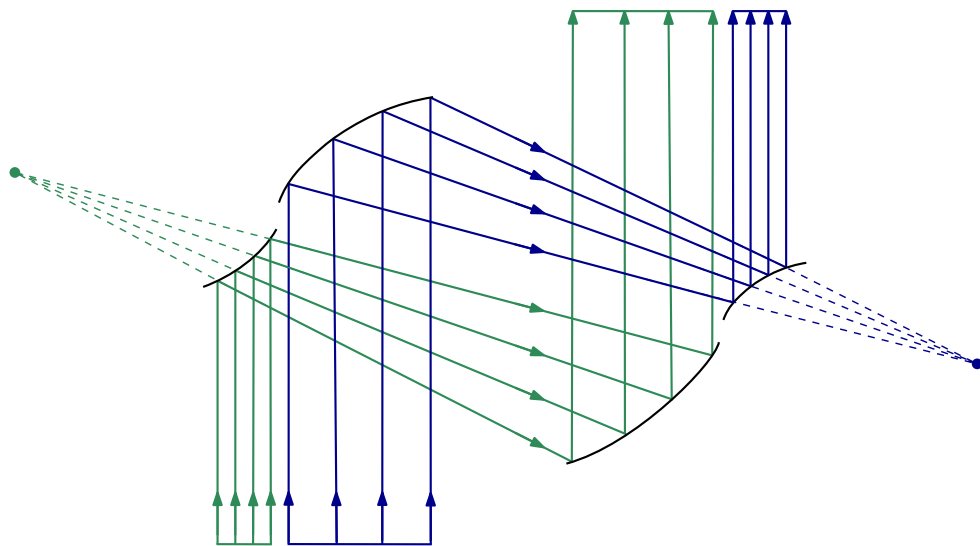


FIGURE 4. Billiard dynamics implementing a right shift. The green and blue rays correspond to the intervals I_k with $k < 0$ and $k \geq 0$, respectively.

Lemma 2. *The read–write operation can be implemented using a billiard.*

Proof. Let δ be the transition function of a Turing machine. Let us consider a computation state encoded by a point $x_{t,k} \in I$, where $t = (t_n)_{n \in \mathbb{Z}}$ is the tape content and $k \in \mathbb{Z}$ is the head position. Suppose that

$$\delta(q, t_k) = (q', s, \varepsilon),$$

so that the read–write operation consists in replacing the symbol t_k by s , while keeping all other symbols unchanged. Then, at the level of the encoding, the read–write operation is equivalent to the mapping

$$x_{t,k} \longmapsto x_{t',k},$$

where $t'_n = t_n$ for $n \neq k$ and $t'_k = s$.

Notice that in other embeddings of Turing machines into dynamical systems, such as those in [25, 26], where the tape is encoded into a two-dimensional Cantor set, the head is assumed to be always at position 0 of the tape. Therefore, the read–write operation involves only the leading ternary digit of the associated point. In our case, however, the symbol t_k that we need to read and possibly modify is stored in a specific digit of the ternary expansion of $x_{t,k}$, namely, in the $(2k + 1)$ -th or $(-2k)$ -th digit when $k \geq 0$ or $k < 0$, respectively. Thus, on the interval $I_k \subset I$ associated with head position k , the admissible computation states split into two alternating families of subintervals, each of them associated with the symbol 0 or 1 at position k . As $|k|$ increases, the number of these intervals grows, while their lengths decrease.

The billiard wall implementing the read–write operation is constructed as a curve whose segments over these subintervals are straight lines with negative or positive slope (depending on whether they correspond to reading a 0 or a 1, respectively). As a result, we can separate the states according to the symbol read and redirect them through different corridors of the billiard, as shown in Figure 5. Moreover, if it is necessary to change a 0 to a 1 (or vice versa), the angle of the straight segments of the wall can be slightly adjusted depending on k , so that the resulting ray is displaced by the required factor.

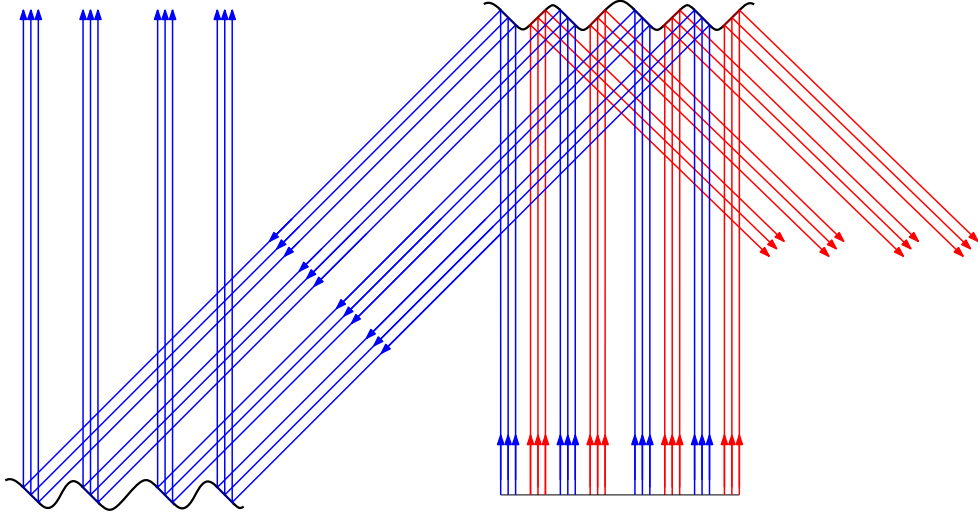


FIGURE 5. Billiard dynamics implementing the read–write operation. The blue and red rays correspond to reading a 0 or a 1, respectively.

Notice that, since there are finite gaps between the intervals where the computation states are, these straight segments can be joined smoothly, producing a differentiable curve.

For a more thorough explanation of how this curve is constructed, refer to the Appendix. □

Remark 3. Notice that the proofs of these two lemmas rely crucially on the specific encoding of the computational state into a one-dimensional interval and the structural features of billiard dynamics. In particular, if one adopted the alternative definition of a Turing machine in which the head is fixed at position zero and the tape is shifted instead, it would suffice to encode the tape t as a single point $x_t \in I$. However, the interval map conjugate to the shift would then be

extremely complicated and, to our understanding, impossible to realize within a physical system. The encoding we use avoids this obstruction at the cost of complicating the read–write map, as discussed in the proof of Lemma 2. Despite this added complexity, the construction remains physically realizable by exploiting the power of billiard dynamics.

Proof of Theorem 2. As discussed above, the strategy of the proof is to translate the directed graph encoding the Turing machine into a planar billiard table whose trajectories simulate its computation.

Using Lemmas 1 and 2, we can construct billiard corridors associated with each edge of the graph so that the billiard dynamics along that corridor implements precisely the read–write–shift operation prescribed by the transition. In this way, whenever a trajectory enters a corridor encoding an edge, the evolution of the tape and head position is updated exactly according to the Turing machine rule corresponding to that edge.

At each state q_i , several edges of the graph may enter the vertex. To reproduce this behavior in the billiard table, we introduce suitable billiard walls, of the same type as those used in the proof of Lemma 2, that merge the incoming corridors into a single outgoing region, as illustrated in Figure 3. The construction is arranged so that if the current computation state is (t, q_i, k) , then the billiard trajectory passes through the point $\iota_i(x_{t,k})$.

The reversibility of the Turing machine is essential at this stage of the construction. The billiard walls used to merge trajectories are designed by reversing the dynamics of the separating walls introduced in Figure 5: rather than splitting a single incoming trajectory into several outgoing ones, they identify several incoming corridors and funnel all corresponding trajectories into a single beam. This is only possible because of reversibility, which ensures that trajectories coming from different edges do not follow the same path.

With this setup, the correspondence between computation and dynamics is exact. The billiard trajectory starting orthogonally at $\iota_0(x_{t,0})$ reaches, again orthogonally to the boundary, the point $\iota_{\text{halt}}(x_{t',k})$ if and only if the Turing machine with input tape t halts with output tape t' and head position k . Therefore, the billiard table simulates the full computation of the machine. In other words, classical two-dimensional billiards can compute. \square

Applying this construction to a universal Turing machine, we get:

Corollary 1. *There exists a two-dimensional billiard table that is Turing complete.*

An interesting outcome of this construction is that the undecidability of the Halting problem [31] implies the undecidability of classical billiard systems. In particular,

Corollary 2. *There exists a two-dimensional billiard table for which deciding whether a given trajectory is periodic is algorithmically undecidable.*

Proof. Let $(B, \iota_0, \iota_{\text{halt}})$ be a computational billiard constructed as in the proof of Theorem 2. It is algorithmically undecidable to determine whether the billiard trajectory starting orthogonally at $\iota_0(x_{t,0})$ is periodic.

By construction, the billiard dynamics simulate the computation of the associated Turing machine with initial tape t . If the machine halts, the trajectory reaches the boundary orthogonally at a point $\iota_{\text{halt}}(x_{t',k})$, where t' is the output tape. The orthogonal reflection reverses the motion, so the trajectory retraces its path and forms a periodic orbit. If the machine does not halt, according to our construction, the trajectory never reaches the halting region but keeps moving around the corridors of the billiard table and never closes up. Since the halting problem is undecidable, so is the problem of deciding whether this billiard trajectory is periodic. \square

4. PHYSICAL APPLICATIONS

Billiard dynamics arises naturally in classical mechanics, either as an exact reformulation of particle systems in configuration space or as a singular limit of smooth Hamiltonian flows. Examples include hard-sphere models in kinetic theory, collision-dominated regimes in celestial mechanics, and systems with steep confining potentials. In this context, the fact that planar

billiards can simulate arbitrary computation has implications beyond idealized reflection models: Turing completeness entails fundamental algorithmic limitations on the long-time prediction of trajectories in physically realizable Hamiltonian systems admitting billiard-type limits.

4.1. Hard-sphere gases and kinetic theory. A system of N hard spheres of radius r moving in a bounded domain $D \subset \mathbb{R}^d$ can be reformulated exactly as a billiard flow in configuration space. Writing $q_i \in D$ for the position of the i th particle, the admissible configuration space is $\mathcal{C} = \{(q_1, \dots, q_N) \in D^N \mid |q_i - q_j| \geq 2r \text{ for all } i \neq j\}$.

Between collisions the dynamics is free, $\ddot{q}_i(t) = 0$, while collisions correspond to elastic reflections on $\partial\mathcal{C}$ [14]. Planar billiards embed as dynamically invariant subsystems of such configuration-space billiards. Consequently, even idealized hard-sphere gas models may contain invariant subsystems whose qualitative dynamics is algorithmically undecidable.

4.2. Collision chains in celestial mechanics. Related structures appear in celestial mechanics through singular limits associated with close encounters. In the Newtonian N -body problem,

$$\ddot{q}_i = \sum_{j \neq i} \frac{m_j(q_j - q_i)}{|q_j - q_i|^3},$$

binary collisions correspond to singularities at $|q_i - q_j| = 0$. In regimes dominated by repeated near-collisions, the motion decomposes into long intervals of nearly Keplerian dynamics separated by short interaction events. Poincaré identified such trajectories as solutions of the second species [27]. This description was later formalized by Bolotin and collaborators [6, 7] through the theory of collision chains, which model near-collision motion using a degenerate billiard approximation in configuration space. Let

$$H(q, p) = \sum_{i=1}^N \frac{|p_i|^2}{2m_i} - \sum_{1 \leq i < j \leq N} \frac{m_i m_j}{|q_i - q_j|}$$

denote the Newtonian Hamiltonian, and let $\Delta_{ij} = \{q \in (\mathbb{R}^3)^N \mid q_i = q_j\}$ be a binary collision manifold. In the degenerate approximation, trajectories consist of Keplerian arcs joined by reflection-type matching conditions at the collision sets Δ_{ij} , arising from stationarity of the Maupertuis action. Collision chains can be characterized as critical points of a discrete Maupertuis action

$$\mathcal{A}(x_0, \dots, x_k) = \sum_{\ell=0}^{k-1} S_E(x_\ell, x_{\ell+1}),$$

where S_E denotes the fixed-energy Kepler action. Under suitable nondegeneracy assumptions, genuine solutions of the N -body problem shadow these trajectories for long times [7, 6].

From a computational perspective, collision chains induce symbolic dynamics based on sequences of near-collisions. In sufficiently complex regimes, this symbolic structure can support algorithmically undecidable qualitative questions about long-time behavior.

4.2.1. Singular perturbation and small-mass limits. Singular perturbation regimes play a central role in celestial mechanics, particularly in small-mass or restricted limits of the N -body problem. In such settings, close encounters generate effective dynamics governed by asymptotic matching across short interaction intervals.

As a schematic model, consider Hamiltonians of the form

$$H_\mu(q, p) = \sum_{i=1}^N \frac{|p_i|^2}{2m_i} - \sum_{1 \leq i < j \leq N} \frac{m_i m_j}{|q_i - q_j|} + \mu V(q), \quad 0 < \mu \ll 1.$$

As $\mu \rightarrow 0$, the dynamics decomposes into long Keplerian arcs separated by brief interaction episodes. In appropriate scaling regimes, this asymptotic behavior is captured by the collision-chain framework [6, 7].

A concrete example is provided by the planar circular restricted three-body problem. After reduction to a rotating frame and rescaling near a close encounter with one primary, the Hamiltonian takes the schematic form

$$H(q, p) = \frac{1}{2}|p - \omega \times q|^2 - \frac{1}{|q|} + \mu V(q) + O(\mu),$$

where the Kepler term dominates near collision and the perturbation $\mu V(q)$ encodes the influence of the distant primary. In the corresponding singular limit, near-collision trajectories satisfy reflection-type matching conditions at the collision set. Symbolic itineraries analogous to those arising in billiard systems then organize the global dynamics.

This perturbative framework explains how billiard-type symbolic dynamics emerges in physically natural Hamiltonian systems, and how sufficiently rich symbolic dynamics can render qualitative questions about long-time behavior algorithmically undecidable.

4.3. Smooth Hamiltonian realizations. Billiard dynamics also appears as a singular limit of smooth Hamiltonian systems with steep confining potentials,

$$H_\varepsilon(q, p) = \frac{1}{2}|p|^2 + V_\varepsilon(q), \quad V_\varepsilon(q) \rightarrow +\infty \text{ as } q \rightarrow \partial B.$$

As $\varepsilon \rightarrow 0$, the Hamiltonian flow converges, away from grazing trajectories, to the billiard flow in B on finite time intervals. This soft-wall approximation embeds billiard dynamics within classical Hamiltonian mechanics and allows undecidability results for billiards to be interpreted as arising in singular limits of smooth, physically natural systems, consistent with the perspective introduced by Moore [25].

5. CONCLUSIONS

Billiard systems have long served as fundamental models in dynamical systems, valued for their simplicity and rich behavior. In this work, we show that their expressive power extends beyond classical notions of integrability and chaos [5, 29]: planar billiards can simulate arbitrary computation. Using the framework of Topological Kleene Field Theory [17], we demonstrate that a billiard table can function as a universal computational device. As a result, basic dynamical questions, including the existence of periodic trajectories become algorithmically undecidable [31, 25]. This viewpoint suggests that computational complexity is intrinsic to billiard dynamics rather than a mathematical artifact. Billiard-type motion arises naturally across physics, often as an effective description in singular or near-collision regimes, notably in celestial mechanics and kinetic theory. In such settings, undecidability imposes fundamental limits on long-term prediction, complementing and extending the traditional role of chaos.

Billiards, therefore, provide a transparent arena for exploring the interface between geometry, dynamics, and computation. An open and provocative question is whether these classical algorithmic barriers survive quantization. If traces of classical undecidability persist in quantum billiards, they would point to limits of predictability that transcend the classical–quantum divide.

REFERENCES

- [1] Rosemary Adejoh, Andreas Jakoby, Sneha Mohanty, and Christian Schindelhauer. How pinball wizards simulate a turing machine. Preprint, arXiv:2510.02560 [cs.CC] (2025), 2025.
- [2] Charles H. Bennett. Logical reversibility of computation. *IBM J. Res. Dev.*, 17:525–532, 1973.
- [3] Michael V. Berry. Regular and irregular semiclassical wavefunctions. *J. Phys. A, Math. Gen.*, 10:2083–2091, 1977.
- [4] George David Birkhoff. *Dynamical Systems*. American Mathematical Society, Providence, 1917.
- [5] George David Birkhoff. On the periodic motions of dynamical systems. *Acta Mathematica*, 50:359–379, 1927.
- [6] Sergey Bolotin. Degenerate billiards in celestial mechanics. *Regular and Chaotic Dynamics*, 22:27–53, 2017.
- [7] Sergey Bolotin and Piero Negrini. Variational approach to second species periodic solutions of poincaré of the three-body problem. *Discrete and Continuous Dynamical Systems*, 33(3):1009–1032, 2013.
- [8] Olivier Bournez, Daniel S. Graça, and Emmanuel Hainry. Computation with perturbed dynamical systems. *J. Comput. Syst. Sci.*, 79(5):714–724, 2013.

- [9] Robert Cardona, Eva Miranda, and Daniel Peralta-Salas. Turing universality of the incompressible Euler equations and a conjecture of Moore. *Int. Math. Res. Not.*, 2022(22):18092–18109, 2022.
- [10] Robert Cardona, Eva Miranda, and Daniel Peralta-Salas. Computability and Beltrami fields in Euclidean space. *J. Math. Pures Appl. (9)*, 169:50–81, 2023.
- [11] Robert Cardona, Eva Miranda, and Daniel Peralta-Salas. Looking at Euler flows through a contact mirror: universality and undecidability. In *European congress of mathematics. Proceedings of the 8th congress, 8ECM, Portorož, Slovenia, June 20–26, 2021*, pages 367–393. EMS Press, Berlin, 2023.
- [12] Robert Cardona, Eva Miranda, and Daniel Peralta-Salas. Towards a Fluid computer. *Found Comput Math*, 25:1921–1937, 2025.
- [13] Robert Cardona, Eva Miranda, Daniel Peralta-Salas, and Francisco Presas. Constructing Turing complete Euler flows in dimension 3. *Proc. Natl. Acad. Sci. USA*, 118(19):9, 2021. Id/No e2026818118.
- [14] Nikolai Chernov and Roberto Markarian. *Chaotic Billiards*, volume 127 of *Mathematical Surveys and Monographs*. American Mathematical Society, 2006.
- [15] Richard P. Feynman. Simulating physics with computers. *International Journal of Theoretical Physics*, 21(6–7):467–488, 1982.
- [16] Edward Fredkin and Tommaso Toffoli. Conservative logic. *Int. J. Theor. Phys.*, 21:219–253, 1982.
- [17] Ángel González-Prieto, Eva Miranda, and Daniel Peralta-Salas. Topological Kleene Field Theories as a model of computation. Preprint, arXiv:2503.16100 [math.DS] (2025), 2025.
- [18] Ángel González-Prieto, Eva Miranda, and Daniel Peralta-Salas. Universality in computable dynamical systems: old and new. *Journal of Physics: Complexity*, 6(3):035014, 2025. Focus Issue on Computation in Dynamical Systems.
- [19] Daniel S. Graça, Manuel L. Campagnolo, and Jorge Buescu. Computability with polynomial differential equations. *Adv. Appl. Math.*, 40(3):330–349, 2008.
- [20] Martin C. Gutzwiller. *Chaos in Classical and Quantum Mechanics*. Springer, 1990.
- [21] F. Haake. *Quantum Signatures of Chaos*. Springer, 3rd edition, 2010.
- [22] Steven Kerckhoff, Howard Masur, and John Smillie. Ergodicity of billiard flows and quadratic differentials. *Annals of Mathematics*, 124(2):293–311, 1986.
- [23] Pascal Koiran, Michel Cosnard, and Max Garzon. Computability with low-dimensional dynamical systems. *Theor. Comput. Sci.*, 132(1–2):113–128, 1994.
- [24] Maryam Mirzakhani. Growth of the number of simple closed geodesics on hyperbolic surfaces. *Annals of Mathematics*, 168(1):97–125, 2008.
- [25] Cristopher Moore. Unpredictability and undecidability in dynamical systems. *Phys. Rev. Lett.*, 64(20):2354–2357, 1990.
- [26] Cristopher Moore. Generalized shifts: Unpredictability and undecidability in dynamical systems. *Nonlinearity*, 4(2):199–230, 1991.
- [27] Henri Poincaré. *Les méthodes nouvelles de la mécanique céleste*, volume III. Gauthier-Villars, Paris, 1899.
- [28] John H. Reif, Justin D. Tygar, and Akitoshi Yoshida. Computability and complexity of ray tracing. *Discrete Comput. Geom.*, 11(3):265–288, 1994.
- [29] Yakov G. Sinai. On the foundations of the ergodic hypothesis for a dynamical system of statistical mechanics. *Soviet Mathematics Doklady*, 4:1818–1822, 1963.
- [30] Terence Tao. On the universality of potential well dynamics. *Dyn. Partial Differ. Equ.*, 14(3):219–238, 2017.
- [31] Alan M. Turing. On computable numbers, with an application to the entscheidungsproblem. *Proc. London Math. Soc.*, 1936.
- [32] Stephen Wolfram. Statistical mechanics of cellular automata. *Rev. Mod. Phys.*, 55(3):601–644, 1983.
- [33] Stephen Wolfram. Undecidability and intractability in theoretical physics. *Phys. Rev. Lett.*, 54:735–738, Feb 1985.
- [34] Stephen Wolfram. Cellular automaton fluids. I: Basic theory. *J. Stat. Phys.*, 45:471–526, 1986.

APPENDIX

The purpose of this appendix is to provide the missing details in the proof of Lemma 2 from the main text, thus completing the argument that the read–write operation can be realized by means of billiard dynamics.

Recall first that, according to our definition of a Turing machine, applying the read–write operation to a computation state (t, k) requires inspecting and possibly modifying the tape symbol t_k . Under our Cantor set–type encoding, this amounts to detecting and, if necessary, changing a specific digit in the ternary expansion associated with the tape before applying the embedding τ_k . For this reason, we argued that, inside the interval I_k corresponding to the head position k , the admissible computation states decompose into two alternating families of

subintervals, depending on whether the symbol at position k is 0 or 1. We now make this decomposition explicit.

Fix $k \in \mathbb{Z}$ and, for simplicity, assume $k \geq 0$ (the case $k < 0$ is completely analogous). We begin by considering the encoding of the tape t alone as a point $x_t \in I$, prior to applying the embedding τ_k . Our goal is to describe two families of Cantor set blocks corresponding to the conditions $t_k = 0$ and $t_k = 1$. Recall that, in our encoding, the symbol t_k is stored in the $(2k+1)$ -th digit of the ternary expansion of x_t . To simplify notation, we introduce

$$x_{\epsilon_1 \dots \epsilon_l} := 2 \sum_{n=1}^l \epsilon_n 3^{-n},$$

where each $\epsilon_n \in \{0, 1\}$.

With this notation, the Cantor set blocks corresponding to tapes with $t_k = 0$ are given by

$$I_{\epsilon_1 \dots \epsilon_{2k} 0} = [x_{\epsilon_1 \dots \epsilon_{2k} 0}, x_{\epsilon_1 \dots \epsilon_{2k} 0} + 3^{-(2k+1)}], \quad \epsilon_n \in \{0, 1\}, \quad n = 1, \dots, 2k,$$

while those corresponding to tapes with $t_k = 1$ are

$$I_{\epsilon_1 \dots \epsilon_{2k} 1} = [x_{\epsilon_1 \dots \epsilon_{2k} 1}, x_{\epsilon_1 \dots \epsilon_{2k} 1} + 3^{-(2k+1)}], \quad \epsilon_n \in \{0, 1\}, \quad n = 1, \dots, 2k.$$

We now apply the embedding τ_k , using its explicit expression from the proof of Lemma 1. Define

$$x_{\epsilon_1 \dots \epsilon_l}^k := \tau_k(x_{\epsilon_1 \dots \epsilon_l}) = 1 + 3^{-(1+k)}(-2 + x_{\epsilon_1 \dots \epsilon_l}).$$

Then the Cantor set blocks inside I_k corresponding to the condition $t_k = s$, with $s \in \{0, 1\}$, are

$$I_{\epsilon_1 \dots \epsilon_{2k} s}^k := \tau_k(I_{\epsilon_1 \dots \epsilon_{2k} s}) = [x_{\epsilon_1 \dots \epsilon_{2k} s}^k, x_{\epsilon_1 \dots \epsilon_{2k} s}^k + 3^{-(3k+2)}],$$

again with $\epsilon_n \in \{0, 1\}$ for $n = 1, \dots, 2k$. There are 2^{2k} such intervals, each of length $3^{-(3k+2)}$.

We now describe the billiard walls implementing the read–write operation. We assume that incoming billiard trajectories move upward, with positive velocity in the y -direction, and have horizontal coordinate $x \in [0, 1]$, where the computation state (t, k) is encoded as $x_{t,k}$. We first treat the case in which no symbol change occurs, so that the goal is simply to distinguish between $t_k = 0$ and $t_k = 1$.

After interacting with the billiard walls, we want trajectories corresponding to $t_k = 0$ to continue vertically with horizontal coordinate $x_{t,k} - 2$, while those corresponding to $t_k = 1$ should continue vertically with horizontal coordinate $x_{t,k} + 2$. To achieve this separation, trajectories first collide with straight walls placed above the intervals $I_{\epsilon_1 \dots \epsilon_{2k} s}^k$, with slope -1 for $s = 0$ and slope $+1$ for $s = 1$.

For $t_k = 0$, we define the walls

$$W_{\epsilon_1 \dots \epsilon_{2k} 0}^k(x) = 2 + x_{\epsilon_1 \dots \epsilon_{2k} 0}^k + \frac{3^{-(3k+2)}}{2} - x, \quad x \in I_{\epsilon_1 \dots \epsilon_{2k} 0}^k.$$

Each such wall is a line segment of slope -1 , centered horizontally above the corresponding interval $I_{\epsilon_1 \dots \epsilon_{2k} 0}^k$ and located at height $y = 2$.

Similarly, for $t_k = 1$, we take walls of slope $+1$ given by

$$W_{\epsilon_1 \dots \epsilon_{2k} 1}^k(x) = 2 - x_{\epsilon_1 \dots \epsilon_{2k} 1}^k - \frac{3^{-(3k+2)}}{2} + x, \quad x \in I_{\epsilon_1 \dots \epsilon_{2k} 1}^k.$$

These walls deflect trajectories corresponding to $t_k = 0$ to the left and those corresponding to $t_k = 1$ to the right.

Once the trajectories have been separated, we must redirect them so that they again travel vertically. For instance, in the case $t_k = 0$, this is achieved by introducing a second family of walls

$$\widetilde{W}_{\epsilon_1 \dots \epsilon_{2k} 0}^k(x) = x_{\epsilon_1 \dots \epsilon_{2k} 0}^k + \frac{3^{-(3k+2)}}{2} - (x + 2),$$

defined for

$$x \in [x_{\epsilon_1 \dots \epsilon_{2k} 0}^k - 2, x_{\epsilon_1 \dots \epsilon_{2k} 0}^k - 2 + 3^{-(3k+2)}].$$

A trajectory starting at $x_{t,k}$ with $t_k = 0$ first reflects off the wall $W_{\epsilon_1 \dots \epsilon_{2k} 0}^k$, then travels along a line of slope -1 until it reaches $\widetilde{W}_{\epsilon_1 \dots \epsilon_{2k} 0}^k$. Since the two walls are parallel, the outgoing trajectory is vertical, with horizontal coordinate $x_{t,k} - 2$, as desired (see Figure 6). A similar construction can be used to have the outgoing trajectory corresponding to $t_k = 1$ travel vertically with horizontal coordinate $x_{t,k} + 2$.

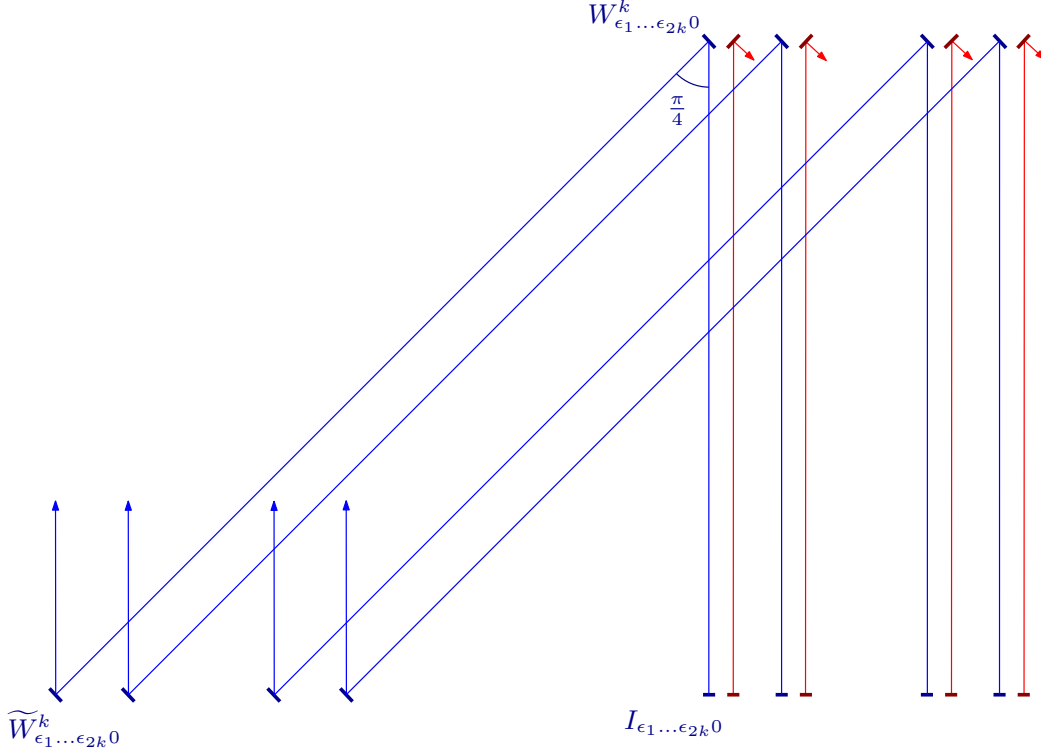


FIGURE 6. Billiard dynamics implementing the read–write operation with no symbol change. The blue and red rays correspond to reading a 0 or a 1, respectively.

We now turn to the case in which a symbol change is required. For simplicity, suppose that we want to modify the tape symbol at position k from $t_k = 0$ to $t'_k = 1$. In terms of our encoding, this means that an incoming vertical trajectory with horizontal coordinate $x_{t,k}$ should be transformed, after interacting with the read–write construction, into a vertical trajectory with horizontal coordinate

$$x_{t,k} + 2 \cdot 3^{-(3k+2)} - 2.$$

Compared with the pure read case, this requires a slight horizontal displacement of the trajectory. Therefore, the separating wall can no longer have slope exactly -1 . Instead, we choose the angle α_k with the horizontal so that

$$\tan \alpha_k = \frac{1}{1 + 3^{-(3k+2)}}.$$

This deviation from slope -1 is very small, especially for large values of k , and in the limit $k \rightarrow \infty$ we recover the original configuration. We can observe this in Figure 7, where the small displacement is displayed compared to the original no-rewrite wall.

We must now verify that all these trajectories travel from the walls $W_{\epsilon_1 \dots \epsilon_{2k} s}^k$ to the corresponding $\widetilde{W}_{\epsilon_1 \dots \epsilon_{2k} s}^k$ without colliding with any other wall. Since all walls lie at the same height, this reduces to checking that, after bouncing off $W_{\epsilon_1 \dots \epsilon_{2k} s}^k$, the trajectory descends sufficiently fast so as not to intersect any other wall $W_{\epsilon'_1 \dots \epsilon'_{2k'} s'}^{k'}$.

Observe first that trajectories corresponding to a symbol change have a steeper downward slope than those in the no-rewrite case. As a result, avoiding collisions is strictly easier in the rewriting case. It therefore suffices to carry out the check for the read–only configuration, where the walls have slopes ± 1 .

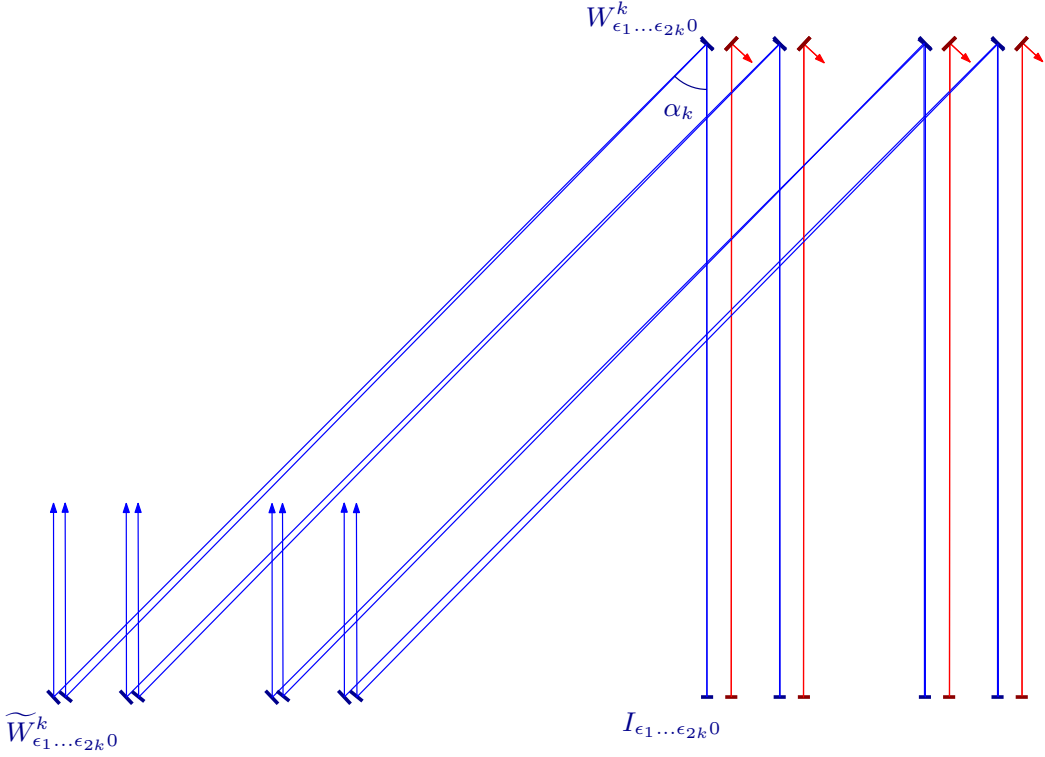


FIGURE 7. Billiard dynamics implementing the read–write operation with symbol change compared to the no-change situation.

Consider a trajectory that bounces off a wall $W_{\epsilon_1 \dots \epsilon_{2k} 0}^k$. Until it reaches $\tilde{W}_{\epsilon_1 \dots \epsilon_{2k} 0}^k$, this trajectory remains parallel to all walls of the form $W_{\epsilon'_1 \dots \epsilon'_{2k'} 1}^{k'}$ (or their slope is larger when the symbol 1 is modified by the transition). Since such walls are separated by a horizontal distance of at least $2 \cdot 3^{-(3k+2)}$, there is no risk of collision with them. We therefore only need to check that the trajectory does not hit any wall $W_{\epsilon'_1 \dots \epsilon'_{2k'} 0}^{k'}$ lying to its left.

It is enough to consider the extremal situation. Namely, we check that the trajectory bouncing off the left endpoint of $W_{\epsilon_1 \dots \epsilon_{2k} 0}^k$, located at

$$(x_{\epsilon_1 \dots \epsilon_{2k} 0}^k, 2 + 3^{-(3k+2)}/2),$$

does not intersect the right endpoint of any wall $W_{\epsilon'_1 \dots \epsilon'_{2k'} 0}^{k'}$, located at

$$(x_{\epsilon'_1 \dots \epsilon'_{2k'} 0}^{k'} + 3^{-(3k'+2)}, 2 - 3^{-(3k'+2)}/2).$$

This amounts to verifying the inequality

$$x_{\epsilon_1 \dots \epsilon_{2k} 0}^k - (x_{\epsilon'_1 \dots \epsilon'_{2k'} 0}^{k'} + 3^{-(3k'+2)}) > \frac{3^{-(3k+2)}}{2} + \frac{3^{-(3k'+2)}}{2}.$$

We first consider the case $k = k'$. By construction, if $x_{\epsilon_1 \dots \epsilon_{2k} 0}^k \neq x_{\epsilon'_1 \dots \epsilon'_{2k'} 0}^{k'}$, then

$$x_{\epsilon_1 \dots \epsilon_{2k} 0}^k - x_{\epsilon'_1 \dots \epsilon'_{2k'} 0}^{k'} \geq 2 \cdot 3^{-(3k+1)}.$$

It follows that

$$x_{\epsilon_1 \dots \epsilon_{2k} 0}^k - (x_{\epsilon'_1 \dots \epsilon'_{2k'} 0}^{k'} + 3^{-(3k+2)}) \geq 3^{-(3k+2)}(6 - 1) > 3^{-(3k+2)},$$

which is more than enough to guarantee the desired separation.

We now turn to the case $k \neq k'$. In this situation, $x_{\epsilon_1 \dots \epsilon_{2k} 0}^k \in I_k$ and $x_{\epsilon'_1 \dots \epsilon'_{2k'} 0}^{k'} \in I_{k'}$. Since the distance between $I_{k'}$ and $I_{k'+1}$ is $3^{-(k'+2)}$, the distance between $I_{k'}$ and I_k is at least this large.

Consequently,

$$x_{\epsilon_1 \dots \epsilon_{2k} 0}^k - (x_{\epsilon'_1 \dots \epsilon'_{2k'} 0}^{k'} + 3^{-(3k'+2)}) \geq 3^{-(k'+2)} \geq 3^{-(3k'+2)} > \frac{3^{-(3k+2)}}{2} + \frac{3^{-(3k'+2)}}{2},$$

where in the last inequality we used the fact that $k > k'$.

We conclude that, after bouncing off $W_{\epsilon_1 \dots \epsilon_{2k} 0}^k$, the trajectory does not intersect any other wall $W_{\epsilon'_1 \dots \epsilon'_{2k'} s'}^{k'}$. By symmetry, the same argument applies to walls of the form $W_{\epsilon_1 \dots \epsilon_{2k} 1}^k$ and to possible collisions with $\tilde{W}_{\epsilon_1 \dots \epsilon_{2k} s}^k$, as well as to the case $k < 0$.

Finally, we note that the estimates used above to rule out unwanted collisions are far from sharp. In particular, they leave plenty of room to connect the straight wall segments by means of smooth bump functions, allowing us to construct a completely smooth billiard wall with a zig-zag profile.

Each straight segment in this zig-zag has vertical size on the order of $3^{-(3k+2)}$, and the total number of such segments is 2^{2k} . As $|k| \rightarrow \infty$, the amplitude of the oscillations therefore tends to zero, while their support occupies an increasingly small portion of the interval I_k . Indeed, the total length of the Cantor blocks of order $2k+1$ (or $2|k|$) vanishes in this limit. Therefore, near the ends of the interval the zig-zag wall converges to a straight line, as shown in Figure 8.

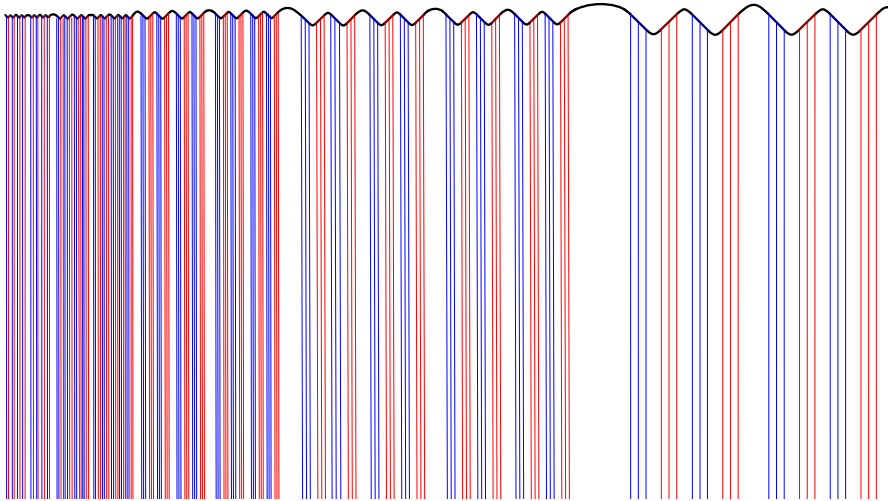


FIGURE 8. How the billiard wall implementing the read–write operation changes as $k \rightarrow -\infty$.

EVA MIRANDA, LABORATORY OF GEOMETRY AND DYNAMICAL SYSTEMS AND SYMCREA RESEARCH UNIT, DEPARTMENT OF MATHEMATICS, UNIVERSITAT POLITÈCNICA DE CATALUNYA, BARCELONA, SPAIN & CENTRE DE RECERCA MATEMÀTICA, CRM & FORSCHUNGSIINSTITUT FÜR MATHEMATIK, ETH ZÜRICH, ZÜRICH, SWITZERLAND

Email address: eva.miranda@upc.edu

ISAAC RAMOS, DEPARTMENT OF MATHEMATICS, ETH ZÜRICH, ZÜRICH, SWITZERLAND & SYMCREA RESEARCH UNIT AT UNIVERSITAT POLITÈCNICA DE CATALUNYA, BARCELONA, SPAIN

Email address: iramos@ethz.ch